Dynamics of the Internal Water Molecules in Squid Rhodopsin

Eduardo Jardón-Valadez,[†] Ana-Nicoleta Bondar,[‡] and Douglas J. Tobias[†*]
[†]Department of Chemistry, University of California, Irvine, CA 92697-2025; and [‡]Department of Physiology and Biophysics, University of California, Irvine, CA 92697-4560

ABSTRACT Understanding the mechanism of G-protein coupled receptors action is of major interest for drug design. The visual rhodopsin is the prototype structure for the family A of G-protein coupled receptors. Upon photoisomerization of the covalently bound retinal chromophore, visual rhodopsins undergo a large-scale conformational change that prepares the receptor for a productive interaction with the G-protein. The mechanism by which the local perturbation of the retinal *cis-trans* isomerization is transmitted throughout the protein is not well understood. The crystal structure of the visual rhodopsin from squid solved recently suggests that a chain of water molecules extending from the retinal toward the cytoplasmic side of the protein may play a role in the signal transduction from the all-*trans* retinal geometry to the activated receptor. As a first step toward understanding the role of water in rhodopsin function, we performed a molecular dynamics simulation of squid rhodopsin embedded in a hydrated bilayer of polyunsaturated lipid molecules. The simulation indicates that the water molecules present in the crystal structure participate in favorable interactions with side chains in the interhelical region and form a persistent hydrogen-bond network in connecting Y315 to W274 via D80.

INTRODUCTION

The recently solved structure of squid rhodopsin (1) reveals that an interhelical cavity is filled by nine water molecules that form a hydrogen-bond (H-bond) network with amino acids D80 and N311. The H-bond network extends up to the phenol group of residue Y315 (Figs. 1 and 4, *A*). Because infrared spectra indicate changes in the vibrational fingerprints of at least eight water molecules upon retinal photoisomerization and formation of the bathorhodopsin state (2), it has been suggested that internal water molecules (IWM) participate directly in transmitting the retinal conformational change to the cytoplasmic side of the protein (1). In the case of bovine rhodopsin, experiments and theory demonstrated that water molecules are important components of the binding pocket (3–6), and the formation of the activated state is accompanied by a significant increase in the number of IWM (7). The interhelical water molecules revealed in the crystal structure of squid rhodopsin hint at a direct role for water-mediated interactions in the activation process.

In the dark state of bovine rhodopsin, the protonated Schiff base of the retinal forms a salt bridge with E113 (4). The precise nature of Schiff base interactions and the role of water molecules in bathorhodopsin have been debated. According to the counterion switch model (8), a H-bond network involving several water molecules and residues, S186, E113, and E181 (4), could serve as a possible pathway for the transfer of a proton from E113 to E181. In an alternative model, which is based on the observation that E113 and E181 are deprotonated in the Meta I and Meta II intermediate states (9), a complex counterion involving E113, E181, and the retinal Schiff base might promote the reorganization of the surrounding H-bonded network between side chains and a water molecule in the activation process (10). Recent NMR experiments and microsecond-timescale molecular dynamics simulations on the dark and Meta I states indicate a threefold increase of the number of IWM in Meta I relative to the dark state and support the complex counterion model (7). Although the increase in the number of IWM upon activation is remarkable, the specific role of the IWM in the activation process of rhodopsin remains unclear.

Understanding the specific role of IWM in the activated state of squid rhodopsin is complicated by the fact that the crystallographic information on water in protein cavities may be affected by artifactual electron densities from protein atoms (11), and additional water molecules absent from the crystal structure could visit the protein transiently (12). Moreover, there could be differences in the distribution and mobility of the IWM in the crystal at 100 K in comparison with a fluid lipid membrane at ambient temperature.

As a first step toward understanding the role of IWM in the propagation of the retinal conformational change, we performed a 20 ns molecular dynamics simulation of squid rhodopsin embedded in a bilayer of polyunsaturated lipids at 300 K. We find that the location and interactions of IWM of squid rhodopsin in the crystal structure are consistent with H-bond networks, showing a particular balance between static and dynamical interactions in the interhelical cavity. Our results suggest a mechanism by which changes in the dynamics of a water chain upon retinal isomerization are transmitted to the protein via changes of the protein-water H-bonds.

MATERIALS AND METHODS

System set up

For the starting coordinates of the protein, we used chain B from the crystal structure of squid rhodopsin (1). Hydrogen atoms were added using the

Submitted December 4, 2008, and accepted for publication December 9, 2008.

*Correspondence: dtobias@uci.edu

Editor: Gregory A. Voth.

0006-3495/09/04/2572/5 $2.00

doi: 10.1016/j.bpj.2008.12.3927

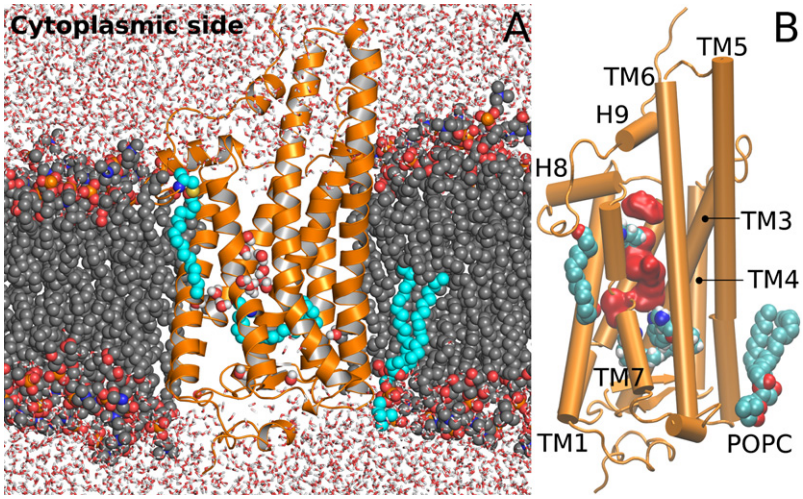

FIGURE 1 (*A*) Final configuration of squid rhodopsin after 20 ns of molecular dynamics simulation. The retinal Schiff base, the POPC molecule, and the carbon atoms of the palmitoyl chain are drawn as cyan spheres. The hydrocarbon chains of the SDPC lipids are depicted as gray spheres, and the lipid headgroups in red, blue, and orange, respectively, for oxygen, nitrogen, and phosphorous atoms. (*B*) Water density isosurface (*red*) for the IWM averaged for the last 15 ns of trajectory. An interhelical water cavity is delimited by retinal and Y315 (*also drawn in spheres*).

PSFGEN tool of the NAMD software (13). All titratable residues were modeled in their standard protonation states. According to the crystal structure, C108 and C186 were disulfide-bridged, and a palmitoyl chain was covalently attached to C337 via a thioester bond. The phosphatidylcholine lipid molecule present in the crystal structure was included as 1-palmitoyl-2-oleoyl-sn-glycero-3-phosphocholine (POPC). The protein was embedded in a bilayer of 241 1-stearoyl-2-docosahexaenoyl-sn-glycero-3-phosphocholine (SDPC) lipids prepared by replicating in the x-y plane a preequilibrated box of 72 SDPC lipids (downloaded from the web site http://persweb.wabash.edu/facstaff/fellers/). The protein-bilayer system was hydrated with 23,705 water molecules. Two chloride ions were added for electroneutrality. A preliminary equilibration was performed for the lipid and bulk water molecules by maintaining the protein and the crystallographic water, POPC, and palmitic acid molecules at their crystal structure coordinates. The constraints on the crystal structure atoms were released in five steps of 200 ps each by gradually decreasing the constraining harmonic potential from 50 to 2 kcal/mol·Å^2, followed by 200 ps simulation with a harmonic constraint of 2 kcal/mol·Å^2 for the retinal heavy atoms, and 1 kcal/mol·Å^2 for all remaining crystal structure heavy atoms. The constraints on all atoms except retinal heavy atoms were then switched off. To ensure that the twisted retinal geometry indicated by the crystal structure is preserved, a constraint of 2 kcal/mol·Å^2 on the retinal heavy atoms for the entire length of the simulation was imposed. The simulation was prolonged to 20 ns.

Computational details

The simulation was performed with the NAMD 2.6 package (13). The CHARMM22 (14) and CHARMM27 (15) force-field parameters were used for the protein and lipids, respectively. Water molecules described with the TIP3P model (16). The retinal parameters optimized for the CHARMM force field were taken from quantum chemical calculations performed by Nina et al. (17). The particle mesh Ewald method (18) was used to calculate the electrostatic interactions with a tolerance of 10^{-6} for the direct part of the Ewald sum, a fourth order interpolation scheme and a grid of $96 \times 96 \times 96$. A multiple time-step scheme was used to integrate the equations of motion with time steps of 4 fs for electrostatic forces, 2 fs for short-range nonbonded interactions, and 1 fs for bonded interactions. All bond lengths involving hydrogen atoms were constrained by using the SHAKE algorithm (19). A Langevin thermostat (13) was used to control the temperature at 300 K, and a Nosé-Hoover-Langevin piston (20) was used to control the pressure at 1 bar.

Trajectory analysis

Root mean-square positional deviation (RMSD) was calculated for the entire 20 ns of trajectory, and the last 15 ns were used for further analysis. The crystal coordinates were considered as the reference structure in all calculations. Root mean-square fluctuations (RMSF) per residue were calculated for the transmembrane (TM1–7) domains, extra-, and intracellular loops, and the cytoplasmic helices (H8–9). By defining a distance cutoff (3.2 to 3.5 Å) from oxygen atoms in the side chains of residues D80, S84, S307, and Y315, all IWM in the crystal structure were located. The number of IWM was tracked during the simulation using a similar distance criterion on selected residues. H-bonds were identified by a geometrical criterion using a cutoff of 3.5 Å and an angle of 50° or less for donor and acceptor pairs. Water survival-time correlation functions (21,22), from which residence times were estimated for IWM in the hydration shell of residues D80, S84, S122, W274, S307, and Y315 were calculated from coordinate frames stored every picosecond. The hydration shell was considered within a distance cutoff of 3.5 Å. Molecular graphics, visual inspection of trajectories, and analysis were performed using the VMD 1.8.6 (23) and PyMOL 0.99 (24) software packages.

RESULTS AND DISCUSSION

The structure of squid rhodopsin was stable during the 20 ns of the simulation. The final configuration of the system is shown in Fig. 1, *A*. The phosphatidylcholine lipid molecule indicated in the crystal structure (modeled here as POPC) remained close to the receptor structure, and the palmitoyl tail attached to C337 is well integrated in the membrane (Fig. 1, *A*). The stability of the structure during the simulation is illustrated by the RMSD from the starting crystal structure coordinates (Fig. 2, *A*). The RMSD converges to a stable average value of 1.57 Å after 5 ns of simulation. RMSF values of Fig. 2, *B* indicate generally larger fluctuations for residues in the aqueous milieu than in the bilayer core, except for EL2 whose low mobility is due to a stable β-sheet structure right next to the binding pocket and facing the extracellular side (Fig. 4, *C*). The cytoplasmic extension of TM5 (from S226 to R240) seems to be more mobile than the solvated domain of TM6. Despite their high mobility (Fig. 2, *B*), the intracellular helices H8-9 conserved their secondary structure that may be important for the recognition of the corresponding G-protein (1,25).

To monitor the behavior of the IWM, we devised an analysis that allows us to identify water molecules present

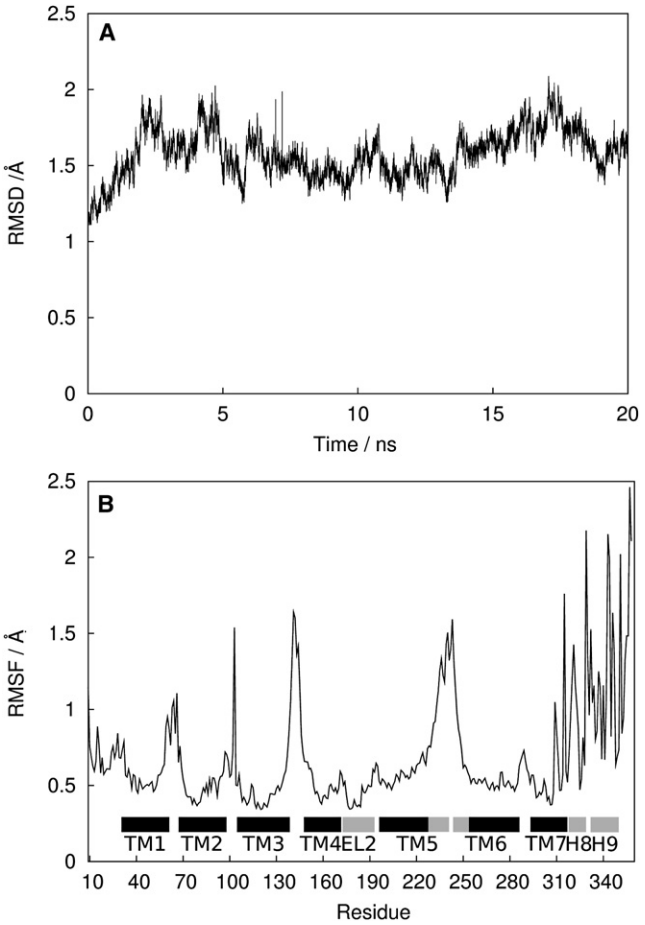

FIGURE 2 (*A*) Positional root mean-square deviation from the crystal structure for all alpha carbons in the squid rhodopsin. After 5 ns of simulation, the receptor structure fluctuates around a stable average of 1.57 Å. (*B*) RMSF per residue for the last 5 ns of trajectory. The TM and EL2 domains are identified according to the amino acid sequence on the *x* axis. Residues in the bilayer core and in the aqueous compartments are identified by black and gray horizontal bars, respectively.

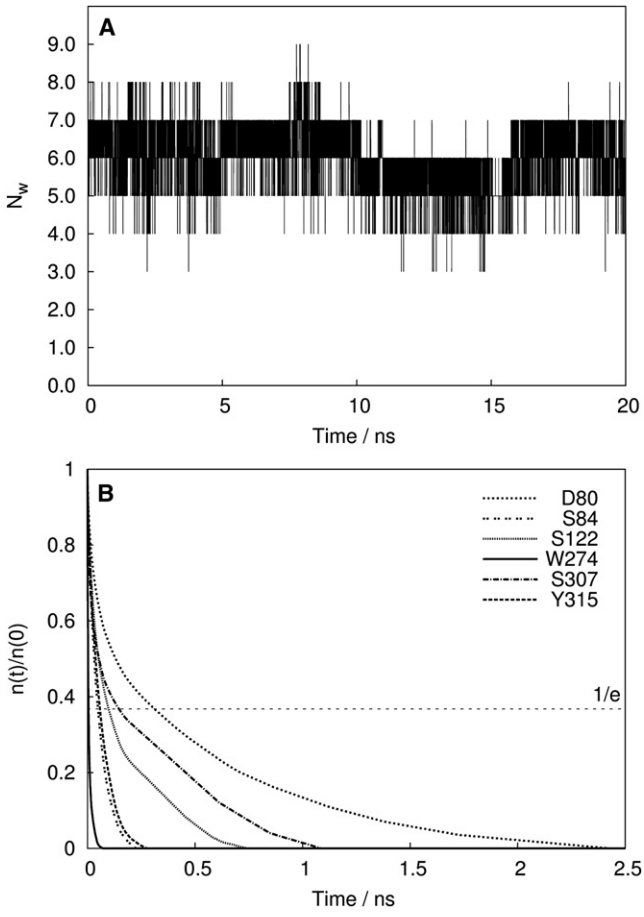

FIGURE 3 (*A*) Number of water molecules (N_w) in the interhelical region as function of simulation time. In the crystal structure, there are nine water molecules in this region of the protein. (*B*) Water survival time correlation functions for the exchange ratio of water molecules in the hydration shell of selected amino acids. n(*t*) is the probability that a water molecule is present in the salvation shell of a particular side chain at time *t* given that is was present at time $t = 0$. Residence times were estimated as the time at which $n(t)/n(0) = 1/e$ (value indicated by the horizontal line).

originally in the crystal structure and the extent to which they remained trapped in the interhelical region during the simulation. Using a distance cutoff criterion, we calculated the distribution of water in the interhelical and derived the water isodensity surface shown in Fig. 1, *B*. The isosurface extends from the retinal binding pocket toward the cytoplasmic side.

To investigate the dynamics of IWM, we identified water molecules within H-bonding distance from protein groups located in the interhelical space from the binding pocket to the cytoplasmic side (D80, W274, and Y315) and measured the time evolution of the number (N_w) of these IWM (Fig. 3, *A*). All nine water molecules present in the crystal structure remained in the interhelical space throughout the simulation, and no exchanges were observed between IWM and intra- or extracellular water molecules. The number of IWM oscillates between 3 and 9, with an average value of 6. D80 has the largest number of IWM (4 to 6) in its vicinity.

The fluctuations of N_w in Fig. 3, *A* are caused by IWM with high mobility. We quantify the mobility in terms of water residence times in the vicinity of particular residues determined from survival time correlation functions (21,22) shown in Fig. 3, *B*. The longest residence time is 311 ps for water molecules close to D80, and the shortest time is 5 ps for water molecules close to W274 (Table 1). The long residence time for D80 is consistent with the strong H-bonding capability of the negatively charged carboxylate group, and perhaps also due to the presence of a polar ring consisting of amino acids

TABLE 1 Residence times of internal water molecules

Residue	D80	S84	S122	W274	S307	Y315
Residence Time/ ps	311	48	98	5	146	58

Estimated residence times (in picoseconds) of the IWM water molecules H-bonding to protein amino acid residues (Fig. 3, *B*). The interaction between the amino acid residues and the IWM is depicted in Fig. 4.

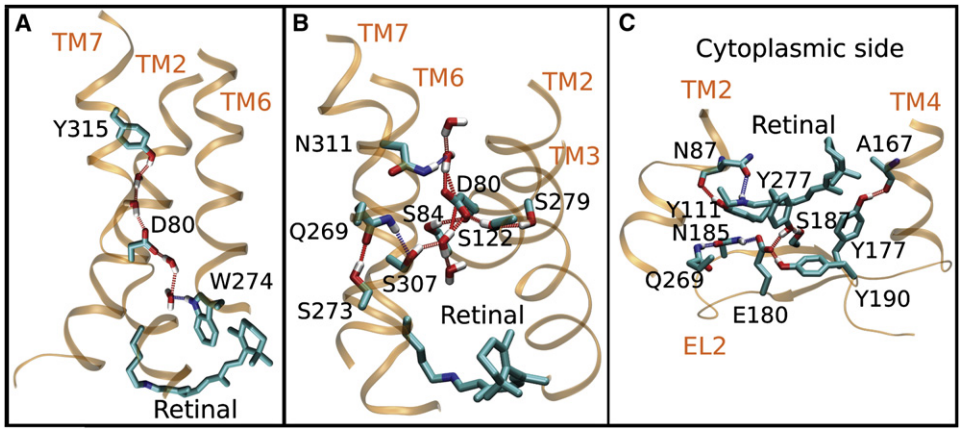

FIGURE 4 H-bonding networks in the interhelical cavity of squid rhodopsin. (*A*) Water-mediated H-bond network from Y315 to W274 involving D80. This H-bond chain was the most recurrent during the trajectory. (*B*) H-bond network involving protein amino acids of a polar ring and IWM. (*C*) H-bond network on the extracellular side of the retinal molecule. EL2 shows a stable β-sheet structure located next to the binding pocket toward the extracellular side.

D80, S84, S122, S79, S273, Q269, and N311 (Fig. 4, *B*). Except for S79, which H-bonds only to S122, the amino acids of the polar ring interact with protein and water molecules (Fig. 4, *B*). Some of the protein-protein H-bonds are stable remaining intact over the duration of the 20 ns of simulation, whereas others break and reform rapidly. For example, H-bonds involving E180 and Y277, N185, or Y190 are stable at average distances of 2.6 Å, 3.4 Å, and 2.7 Å, respectively. In contrast, the D80 sidechain switches between H-bonds with S122 and N311 on the 100 ps time scale.

The details of the mechanism leading to signal transduction by squid rhodopsin are not known. It is also not clear whether the IWM contribute to the propagation of the conformational change from the retinal site to the cytoplasmic region of the protein. By defining the oxygen atom of the phenol group in Y315 as starting point, and considering several atoms in the binding pocket as endpoints, we identified a H-bond network between Y315 and W274, mediated by D80 and four water molecules, as the shortest H-bond path involving IWM (Fig. 4, *A*). This H-bond chain was the most recurrent in the simulation. It is conceivable that isomerization of the retinal could lead to changes in side-chain conformations and/or H-bonds involving water molecules that would distort or disrupt this H-bond network. Perturbation of the water molecules in the H-bond network can lead to changes of the H-bonding between the water molecules and the amino acids of the polar ring and of the interactions between amino acids of the polar ring (Fig. 4, *B*). These changes can further induce changes in the dynamics of transmembrane helices TM2, TM3, TM6, and TM7, which contribute the amino acids part of the polar ring. Isomerization-induced changes in protein dynamics could also be propagated via the network of H-bonds observed on the extracellular side of the retinal (Fig. 4, *C*). Isomerization of the retinal likely perturbs the H-bond between the Schiff base and N87, whose carbonyl group H-bonds with Y111. Given the proximity between Y111 and the network of H-bonds comprising amino acids of the EL2 and TM4, changes in the dynamics of Y111 could be propagated, via the extracellular H-bond network (Fig. 4, *C*), to TM4.

This work was supported by the National Science Fundation (grant CHE-0750175 to D.J.T).

The authors are grateful to Professors Midori Murakami and Tsutomu Kouyama for providing the original crystal structure before publication. E.J.-V. is a posdtoctoral fellow supported by Consejo Nacional de Ciencia y Tecnología, Mexico. E.J.-V. is indebted to the Theory and Experiments on Membrane Protein Organization group of the University of California, Irvine for hospitality and for providing valuable analysis tools and fruitful discussions. A.-N.B. is supported by grants from the National Institutes of Health (GM74637and GM68002).

REFERENCES

1. Murakami, M., and T. Kouyama. 2008. Crystal structure of squid rhodopsin. *Nature*. 453:363–367.
2. Ota, T., Y. Furutani, A. Terakita, Y. Shichida, and H. Kandori. 2006. Structural changes in the Schiff base region of squid rhodopsin upon photoisomerization studied by low-temperature FTIR spectroscopy. *Biochemistry*. 45:2845–2851.
3. Borhan, B., M. L. Souto, H. Imai, Y. Shichida, and K. Nakanishi. 2000. Movement of retinal along the visual transduction path. *Science*. 288:2209–2212.
4. Okada, T., M. Sugihara, A.-N. Bondar, M. Elstner, P. Entel, et al. 2004. The retinal conformation and its environment in rhodopsin in light of a new 2.2 Å crystal structure. *J. Mol. Biol.* 342:571–583.
5. Mizuide, N., M. Shibata, N. Friedman, M. Sheves, M. Belenky, et al. 2006. Structural changes in bacteriorhodopsin following retinal photoisomerization from the 13-cis form. *Biochemistry*. 45:10674–10681.
6. Struts, A. V., G. F. J. Salgado, K. Tanaka, S. Krane, K. Nakanishi, et al. 2007. Structural analysis and dynamics of retinal chromophore in dark and Meta I states of rhodopsin from 2H NMR of aligned membranes. *J. Mol. Biol.* 372:50–66.
7. Grossfield, A., M. C. Pitman, S. E. Feller, O. Soubias, and K. Gawrisch. 2008. Internal hydration increases during activation of the G-protein-coupled receptor rhodopsin. *J. Mol. Biol.* 381:478–486.
8. Yan, E. C. Y., M. A. Kazmi, Z. Ganim, J.-M. Hou, D. Pan, et al. 2003. Retinal counterion switch in the photoactivation of the G protein--coupled receptor rhodopsin. *Proc. Natl. Acad. Sci. USA*. 100: 9262–9267.
9. Lüdeke, S., M. Beck, E. C. Y. Yan, T. P. Sakmar, F. Siebert, et al. 2005. The role of Glu181 in the photoactivation of rhodopsin. *J. Mol. Biol.* 353:345–356.
10. Okada, T., Y. Fujiyoshi, M. Silow, J. Navarro, E. M. Landau, et al. 2002. Functional role of internal water molecules in rhodopsin revealed by x-ray crystallography. *Proc. Natl. Acad. Sci. USA*. 99: 5982–5987.

11. Quillin, M. L., P. T. Winfield, and B. W. Matthews. 2006. Determination of solvent content in cavities in IL-1β using experimentally phased electron density. *Proc. Natl. Acad. Sci. USA.* 103:19749–19753.

12. Grudinin, S., G. Büldt, V. Gordeliy, and A. Baumgaertner. 2005. Water molecules and hydrogen bonded networks in the bacteriorhodopsin-molecular dynamics simulations of the ground state and the M-intermediate. *Biophys. J.* 88:3252–3261.

13. Phillips, J. C., R. Broun, W. Wang, J. Gumbart, E. Tajkhorshid, et al. 2005. Scalable molecular dynamics with NAMD. *J. Comput. Chem.* 26:1781–1802.

14. MacKerell, A. D., D. Bashford, M. Bellott, R. L. Dunbrack, J. D. Evanseck, et al. 1998. All-atom empirical potential for molecular modeling and dynamics studies of proteins. *J. Phys. Chem. B.* 102:3586–3616.

15. Feller, S. E., K. Gawrisch, and .A. D. MacKerell Jr. 2002. Polyunsaturated fatty acids in lipid bilayers: Intrinsic and environmental contributions to their unique physical properties. *J. Am. Chem. Soc.* 124: 318–326.

16. Jorgensen, W. L., J. Chandrasekhar, J. D. Madura, R. W. Impey, and M. L. Klein. 1983. Comparison of simple potential functions for simulating liquid water. *J. Chem. Phys.* 79:926–935.

17. Nina, M., B. Roux, and J. C. Smith. 1995. Functional interactions in bacteriorhodopsin: a theoretical analysis of retinal hydrogen bonding with water. *Biophys. J.* 68:25–39.

18. Darden, T., D. York, and L. Pedersen. 1993. Particle mesh Ewald – an Nlog(N) method for Ewald sums in large systems. *J. Chem. Phys.* 98:10089–10092.

19. Ryckaert, J. P., G. Ciccotti, and H. J. C. Berendsen. 1977. Numerical-integration of cartesian equations of motion of a system with constraints-molecular-dynamics of n-alkanes. *J. Comput. Phys.* 23: 327–341.

20. Feller, S. E., Y. Zhang, and R. W. Pastor. 1995. Constant pressure molecular dynamics simulation: the Langevin piston method. *J. Chem. Phys.* 103:4613–4621.

21. Impey, R. W., P. A. Madden, and I. R. McDonald. 1993. Hydration and mobility of ions in solution. *J. Chem. Phys.* 87:5071–5083.

22. Freites, J. A., D. J. Tobias, G. von Heijne, and S. H. White. 2005. Interface connections of a transmembrane voltage sensor. *Proc. Natl. Acad. Sci. USA.* 102:15059–15064.

23. Humphrey, W., A. Dalke, and K. Schulten. 1996. VMD: visual molecular dynamics. *J. Mol. Graph.* 14:33–38.

24. DeLano, W. L. 2002. The PyMOL Molecular Graphics System DeLano Scientific, San Carlos, CA, USA.

25. Scheerer, P., J. H. Park, P. W. Hildebrand, Y. J. Kim, N. Kraub, et al. 2008. Crystal structure of opsin in its G-protein-interacting conformation. *Nature.* 455:497–502.